Journal of Applied Polymer Science

Optimization of the silane treatment of cellulosic fibers from eucalyptus wood using response surface methodology

Ester Rojo, M. Virginia Alonso, Belén Del Saz-Orozco, Mercedes Oliet, Francisco Rodriguez
Department of Chemical Engineering, Complutense University of Madrid, 28040 Madrid, Spain
Correspondence to: E. Rojo (E-mail: erojorec@quim.ucm.es)

ABSTRACT: Viscose cellulosic fibers from eucalyptus wood were treated with organosilanes to introduce specific functionalities on the fibers and enhance their wettability and adhesion with phenolic matrices in composites. Modeling procedures were employed to optimize the conditions of the treatments of the fibers with the silanes (3-aminopropyl) trimethoxysilane (APS) and 3-(2-aminoethylamino) propyltrimethoxysilane (AAPS). The analyzed responses were relative intensities of the bands 1565/897 and 1120/897 cm^{-1}, measured by Fourier transform infrared spectroscopy, and the silicon amount incorporated into the cellulosic fibers, which was determined by energy dispersive X-ray analysis. In addition, surface morphology of the silane treated fibers was observed using scanning electron microscopy. The treatments of the cellulosic fibers with 2.2% APS for 120 min and 1.5% AAPS for 100 min were selected as optimums. According to contact angle measurements, both treatments enhanced the wettability between the fibers and a resol-type phenolic resin, revealing the possible use of the silane treated fibers as reinforcement in phenolic composites. © 2015 Wiley Periodicals, Inc. J. Appl. Polym. Sci. **2015**, *132*, 42157.

KEYWORDS: cellulose and other wood products; fibers; properties and characterization; silane treatment; surface modification

Received 25 November 2014; accepted 2 March 2015
DOI: 10.1002/app.42157

INTRODUCTION

Development of new reinforced composites based on renewable resources has increased during the last few years as a result of a greater environmental awareness. Cellulose is the most abundant biopolymer in nature, which can be found as hairs (cotton, kapok), bast (flax, hemp, jute, ramie), and hard-fibers (sisal, henequen, coir). Several authors have reviewed the behavior of cellulosic fibers-reinforced composite materials.[1–6] Experimental design has been recently applied by our group to analyze the behavior of phenolic composites.[7,8] Statistical models were developed to describe the tensile and flexural properties of cellulosic fiber-reinforced phenolic composites and the effects of simple variables such as time and temperature on the elongation, strain energy density, modulus, and strength were investigated. In addition, the influence of fiber loading on the properties of the final composites was studied.

Cellulosic fibers are more resistant to the absorption of noise, lighter, and lower cost than glass fibers, which are the most used fibers in reinforced composites. In addition, cellulosic fibers can be recycled and obtained using significantly less energy. However, poor resistance to moisture absorption and bad adhesion limit the use of the cellulosic fibers as reinforcement in composites. The high hydrophilic nature of the cellulosic fibers adversely affects their compatibility with hydrophobic matrices and it may cause a loss of bond strength even with hydrophilic polymers.[9] Surface modification of the fibers reduces their hydrophilicity and improves the fiber-matrix adhesion in composites. Several fibers' treatments have been extensively reviewed in the literature, including reaction with acid compounds and anhydrides, coupling with organosilanes, chemical grafting, as well as the surface activation of the fibers by physical agents.[1,4,10–16] In a previous work, alkali treatment was applied to viscose cellulosic fibers from eucalyptus wood to improve the surface properties of the fibers for using as reinforcement in phenolic composites.[17] In the present work, effects of different silane treatments on the cellulosic fibers were studied.

Surface treatment of the fibers with functional trialkoxysilanes, $R'Si(OR)_3$, is one of the most efficient chemical methods because of the special structure of these silanes.[18,19] Trialkoxysilanes act as coupling agents between fibers and matrices in composites and improve the bonding at the interface. Moreover, these silanes make the fibers more hydrophobic and limit the moisture absorption. The mechanisms of the coupling reactions are related to the presence of two types of reactive moieties in the structure of the trialkoxysilanes. On one hand, the siloxane alkoxy groups Si—OR result in Si—OH groups when water is present in the reaction medium. After that, Si—OH groups enable the silane through C—O—Si bonds to be chemically bonded

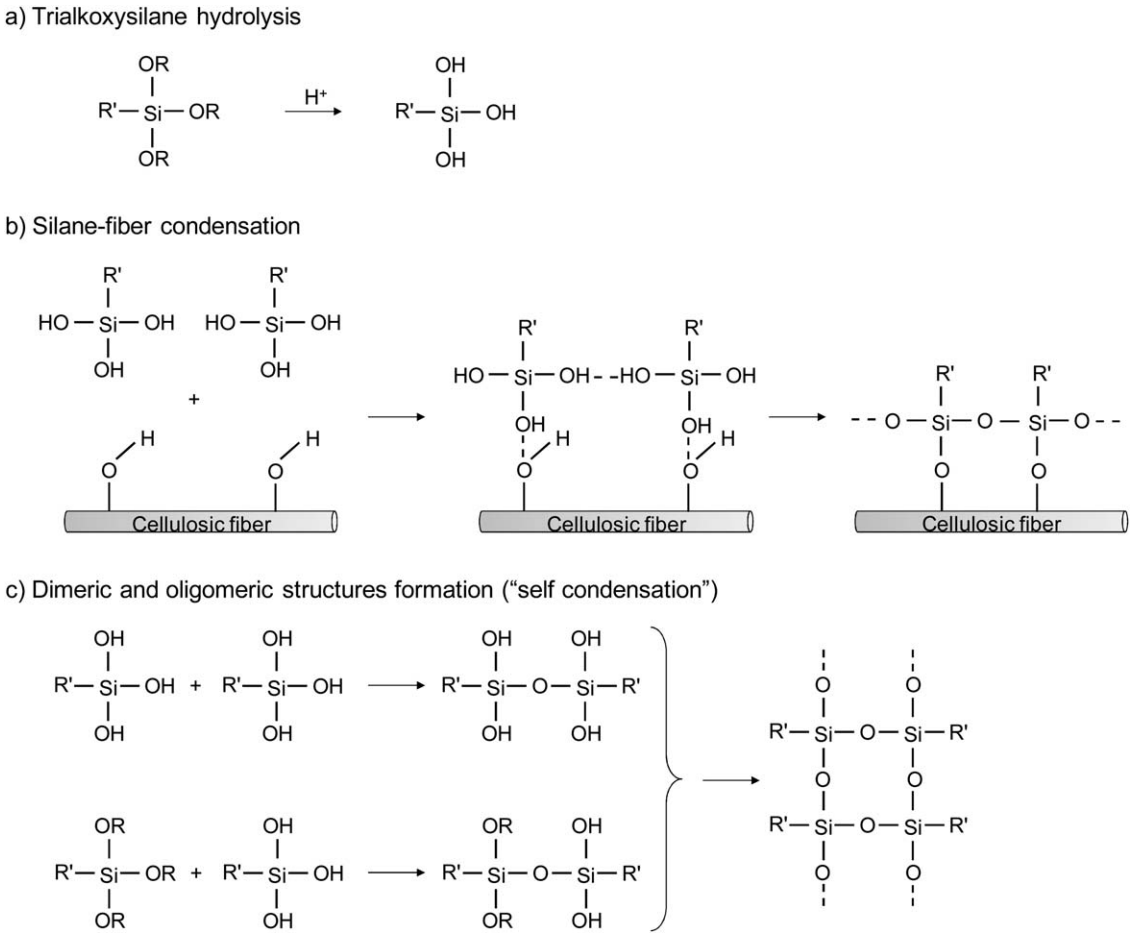

Figure 1. Reactions during the treatment of cellulosic fibers with silanes.

to the cellulose hydroxyls.[1] On the other hand, the organic functionality *R′* (amine, vinylic, etc.) is able to copolymerize with organic matrices. Selection of a silane with an organic functionality compatible with the matrix is essential for the efficiency of the treatment. Different amino silanes have been successfully used for various matrices, such as epoxy resin,[20–23] phenolic resin,[24] polyethylene,[25] polylactic acid,[26] PVC,[27] or unsaturated polyester.[22]

Reactions taking place during the silane treatment of cellulosic fibers are shown in Figure 1. First, the hydrolysis of the trialkoxysilane in acid aqueous medium results in the corresponding silanol derivative $R'Si(OH)_3$ [Figure 1(a)].[28–30] The hydroxyl groups of the hydrolyzed silane are oriented towards the hydroxyl groups of the cellulosic fibers and then condensation takes place with the subsequent detachment of water [Figure 1(b)].[30–32] This is the real bonding between silane and fiber, which has as a result the formation of covalent Si—O—C bonds. The free silanols also absorb and react with each other forming a rigid polysiloxane structure.[19] The problem is that several undesired reactions may occur at the same time that the silane-fiber condensation because the partially or totally hydrolyzed silanes in the aqueous medium constitute a rather reactive system. Condensation reactions of the silanol groups both with each other and with the alkoxy groups of the nonhydrolyzed silane result in dimeric and oligomeric structures, respectively, and may cause the system to evolve over time [Figure 1(c)].[33–35] The condensation should be minimized at this stage to leave the silanols free for being adsorbed to the hydroxyl groups in the cellulosic fibers.[19,30–32]

Regenerated cellulosic fibers possess high purity, uniformity, and reproducibility of properties, which make them attractive for the use as reinforcement in composites.[36] Commercial regenerated cellulosic fibers are manufactured using the xanthate derivatisation process (viscose) or the *N*-methyl-morpholine-*N*-oxide (NMMO) dissolution process (lyocell). Viscose fibers are the most available and widely used regenerated cellulosic fibers and for these reasons they have been selected in the present study.[37–40]

In this work, surface modifications of viscose cellulosic fibers from eucalyptus wood with (3-aminopropyl) trimethoxysilane (APS) and 3-(2-aminoethylamino) propyltrimethoxysilane (AAPS) were studied. Both organosilanes were used to provide the fibers with specific functionalities and enhance their wettability with phenolic matrices in composites. A central factorial design was applied to each silane and optimal conditions of the treatments were selected after studying the variables silane concentration and soaking time. Progresses in the modifications were followed through structural changes of the fibers (FTIR)

and the silicon amount incorporated into the fibers (EDS). In addition, surface morphology of the silane treated fibers was observed (SEM) and wettability between the fibers and a resol-type phenolic resin was studied by contact angle measurements.

EXPERIMENTAL

Materials

Viscose cellulosic fibers from eucalyptus wood were supplied by Sniace (Spain). Linear density and length of the fibers were 1.7 dtex (0.17 g/1000 m) and 1.7–38 mm, respectively. The organosilanes (3-aminopropyl) trimethoxysilane (APS) and 3-(2-aminoethylamino) propyltrimethoxysilane (AAPS) were used in the surface treatment of the cellulosic fibers and were provided by Sigma-Aldrich®.

Ethanol and glacial acetic acid from Panreac Química, S.A.U. were used for preparing the hydrolysis silanes medium and adjusting the pH, respectively. Spectroscopic grade potassium bromide (Scharlau Chemie) was used to prepare the FTIR pellet samples. A resol-type phenolic resin supplied by Momentive Specialty Chemicals was used in the contact angle measurements.

Silane Treatment

First, an amount of silane (varying in the ranges 1–4% for the APS and 0.5–3% for the AAPS) was hydrolyzed using an acidified 80/20 wt/wt ethanol/water medium at 30°C. The pH of the solution was adjusted to 3.5 with acetic acid and continuous stirring was applied during 30 min for the complete hydrolysis of the silanes. Then, the fibers were soaked in the solutions and kept under stirring during a given time (in the range 30–180 min). The fibers were further washed and finally dried in an oven at 60°C for 24 h.

Fourier Transform Infrared Spectroscopy Analysis (FTIR)

FTIR was employed to analyze the structural changes in the cellulosic fibers after the treatments. FTIR spectra were recorded with a Mattson Satellite 5000 Spectrophotometer, using the KBr pellet method. Samples of the finely divided cellulosic fibers (1 mg) were dispersed in a matrix of KBr (99 mg). The pellets were then formed by compression at 7 t for 30 s. The acquisitions conditions were: spectral width of 4000–400 cm^{-1}, 32 scans and 2 cm^{-1} resolution. The relative intensities of FTIR bands 1565/897 and 1120/897 cm^{-1} ($I_{1565/897}$ and $I_{1120/897}$) were determined to follow the progress of the reactions during the silane treatments of the cellulosic fibers.

Energy Dispersive X-ray Analysis (EDS) and Scanning Electron Microscopy (SEM)

The scanning electron microscope JEOL JM-6400 with an energy-dispersive X-ray (EDS) detector was used to measure the semi-quantitative amount of silicon incorporated into the cellulosic fibers after the treatment (*Si*). For EDS analysis, cellulosic fibers were fixed with double-sided adhesive tape over specimen stubs of 12.5 mm diameter [Figure 2(a)]. The operation voltage of the microscope was 40 kV.

The scanning electron microscope (SEM) was also used to observe the surface morphology of the cellulosic fibers. Samples for the SEM observations were prepared according to the scheme of Figure 2(b). In this case, the sample surfaces were sputtered with graphite and gold to enhance electrical conductivity.

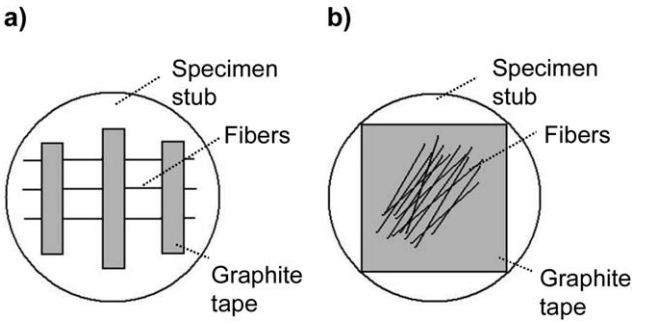

Figure 2. Scheme of the sample preparation for the JEOL JM-6400 analysis: (a) EDS and (b) SEM samples.

Contact Angle Measurements

Contact angles between a resol-type phenolic resin and the cellulosic fibers were measured using the sessile drop method with a Dataphysics OCA-20 contact angle analyzer. The drop images were processed with the SCA 20.2.0 software, which calculated both the left and right contact angles from the shape of the drop with an accuracy of ±0.1°.

Experimental Design and Statistical Analysis

Experimental design is a useful statistical tool that allows analyzing simultaneously the effects of different variables (factors) on the properties of a system (responses). In the present work, two central composite experimental designs were applied to optimize the conditions of the treatments of the cellulosic fibers with the silanes APS and AAPS. Each experimental design involved two factors at two levels, designated by 2^2 (11 runs: $2^2 + 3$ central points + 4 star points). The studied factors were silane concentration (c) and soaking time of the fibers in the silane solutions (t). Ranges for these variables were established in preliminary experiments and they were: 1–4% and 30–180 min in the APS design and 0.5–3% and 30–180 min in the AAPS design. Experimental conditions of the mentioned designs are summarized in Table I.

Data processing was accomplished using *Statgraphics Centurion XV*, which enables one to apply analysis of variance (ANOVA) and multiple linear regression methods. A quadratic model capable of fitting the experimental data was obtained for each response [eq. (1)].

$$Z = a_0 + a_1 \times X_1 + a_2 \times X_2 + a_{12} \times X_1 \times X_2 + a_{11} \times X_1^2 + a_{22} \times X_2^2 \quad (1)$$

where Z is the predicted response, a_0 is a constant interception coefficient, a_1 and a_2 are the linear coefficients, a_{12} is a cross-product coefficient, a_{11} and a_{22} are the quadratic coefficients, and X_1 and X_2 are the studied factors.

The analyzed responses were the relative intensities of FTIR bands $I_{1565/897}$ and $I_{1120/897}$ and the percentage of silicon (*Si*) in the cellulosic fibers determined by EDS. Each response was further plotted as a contour map (two-dimensional response surface) to graphically study the influence of the factors silane concentration and soaking time.

Table I. Experimental Conditions and Results for Cellulosic Fibers Treated with APS and AAPS Silanes

	APS design					AAPS design				
Run	c (%)	t (min)	$I_{1565/897}$	$I_{1120/897}$	*Si* (%)	c (%)	t (min)	$I_{1565/897}$	$I_{1120/897}$	Si (%)
1	2.5	105	1.221	0.923	0.52	3.0	30	1.220	0.946	0.31
2	4.6	105	1.538	1.006	1.25	1.7	0	0.756	0.895	0
3	4.0	30	1.399	0.984	0.83	0.5	30	0.924	0.892	0.12
4	0.4	105	0.907	0.904	0.10	3.5	105	1.387	0.951	0.97
5	4.0	180	1.381	0.989	0.85	1.7	105	1.185	0.929	0.16
6	2.5	105	1.171	0.927	0.55	0.5	180	0.936	0.900	0.06
7	1.0	180	0.890	0.905	0.13	1.7	105	1.185	0.937	0.21
8	1.0	30	0.784	0.875	0.11	3.0	180	1.397	0.951	0.89
9	2.5	105	1.218	0.919	0.48	0	105	0.752	0.892	0
10	2.5	211	1.047	0.935	0.60	1.7	211	1.211	0.922	0.53
11	2.5	0	0.763	0.886	0	1.7	105	1.173	0.929	0.29

RESULTS AND DISCUSSION

Full Experimental Design

The results of the central factorial designs applied to the study of the APS and AAPS treatments were included in Table I. Values of the responses variables ($I_{1565/897}$, $I_{1120/897}$, and *Si*) were fitted to quadratic models as functions of the independent variables, according to eq. (1). Regression coefficients of the models and a summary of the ANOVA analysis are given in Table II. Each effect had a probability (*P*-value) and an F distribution (*F*-test), which indicated its significance. Nonsignificant effects for a confidence level of 95% (*P*-value >0.05% and/or *F*-test < 18.51) were excluded and statistically significant models were obtained.

Determination coefficients (R^2) were in the range 93.95–97.49%, which means that the applied models explained adequately the data variation. Standard errors of the estimates (SEE) and mean absolute errors (MAE) were also included in Table II, and they represent the standard deviations of the residuals and the average values of the residuals, respectively. In addition, the ratio pure error sum of squares/total sum of squares (SSE/SST) was calculated and values between 0.0002 and 0.0075 were obtained. The small values of the SSE/SST revealed that the process variables were well controlled during the experiments and that the experimental errors were minimal.

FTIR Analysis

The relative intensities of FTIR bands $I_{1565/897}$ and $I_{1120/897}$ were studied. The band intensity 897 cm^{-1} was taken as a reference in the two responses. This band is characteristic of the symmetric stretching in plane γ (COC) of the cellulose (β-glycosidic bond), and it is not affected by the silane treatment of the fibers.[41,42] Infrared spectra in the 4000–400 cm^{-1} region of the raw fibers and the fibers treated with the APS and AAPS silanes at the central points of the experimental designs are shown as examples in Figure 3.

The relative intensity $I_{1565/897}$ reports the amount of silane bonded to the fibers after the treatment. The band near 1565 cm^{-1} is characteristic of the deformation of the NH_2 groups, which are contained within the APS and AAPS amino silanes.[32,43] The appearance of this band in the spectra of the treated fibers (Figure 3) supports the presence of the APS and AAPS silanes in the fibers, which is difficult to assess by other methods. The $I_{1565/897}$ values of the APS and AAPS silane treated fibers were in the ranges 0.763–1.538 and 0.752–1.397, respectively, as shown in Table I. The lowest values of this response belong to the untreated fibers and the highest values to the treated with the highest concentrations of silanes (4.6% in the APS design and 3.5% in the AAPS design).

The contour maps for the relative intensity $I_{1565/897}$ of the APS and AAPS silane treated fibers are shown in Figure 4(a,b), respectively. It can be appreciated that the amount of silane bonded to the fibers after the treatments ($I_{1565/897}$) is more affected by the APS or AAPS silane concentrations than by the soaking time of the fibers in the respective silane solutions. Increasing the concentration of any silane produces the growth of the relative intensity $I_{1565/897}$. An increase in the soaking time of the cellulosic fibers in the APS silane solutions leads to the rise of $I_{1565/897}$ up to a maximum, which is reached at 120 min. Above this time, the $I_{1565/897}$ is reduced due to reversible hydrolysis, which strips part of the silane off the fiber surface.[44] Increasing the soaking time of the fibers in the AAPS silane solutions produces the growth of $I_{1565/897}$ up to an approximately constant value, different for each silane concentration. In this case, there is no evidence that the reversible hydrolysis occurs.

The relative intensity $I_{1120/897}$ has been chosen for controlling the self condensation reactions that can take place during the silane treatment of the fibers [Figure 1(c)]. Thus, the intensification of the relative intensity $I_{1120/897}$ represents the nondesirable formation of dimeric and oligomeric structures. The band near 1120 cm^{-1} is characteristic of the stretching of the —Si—O—Si— bonds. These bonds are formed during the silane-fiber condensation [Figure 1(b)]. However, the intensification of the band occurs when undesired self condensation reactions take place [Figure 1(c)] and dimeric and oligomeric structures are formed by reacting silanol groups both with each other and with alcoxi groups of nonhydrolyzed silane, respectively.[29,32,43,45–47]

Table II. Regression Coefficients and Analysis of Variance for the Responses Studied

Coefficients and ANOVA	$I_{1565/897}$		$I_{1120/897}$		*Si* (%)	
	APS	AAPS	APS	AAPS	APS	AAPS
Regression coefficients						
a_0	0.43607	0.711273	0.882722	0.869418	−0.280138	0.143339
a_1 (*c*)	0.16736	0.218294	−0.0144794	0.01877	0.0809934	−0.210139
a_2 (*t*)	0.00621128	0.00159945	0.000175161	0.000414849	0.00562921	−0.000870778
a_{11} (c^2)	-	−0.0283252	0.00853683	-	0.0351481	0.00771763
a_{22} (t^2)	−0.0000256319	−0.00000686294	-	−0.00000155835	−0.0000197054	-
a_{12} ($c{\cdot}t$)	-	0.000441624	-	-	-	0.00170667
ANOVA						
P-values[a]	<0.0248	<0.0053	<0.0099	<0.0472	<0.0341	<0.0447
F-test[b]	>38.80	>188.87	>99.58	>19.69	>27.83	>20.91
R^2	95.38	97.49	95.66	93.77	93.95	97.05
SEE	0.0281	0.0060	0.0037	0.0042	0.0351	0.0656
MAE	0.0372	0.0227	0.0071	0.0044	0.0766	0.0487
SSE/SST	0.0023	0.0002	0.0015	0.0063	0.0016	0.0075

( ) Factor accompanying the regression coefficient in the model.
- Lack of significant coefficient.
[a] The highest *P*-value of all the effects in each model is shown.
[b] The lowest *F*-test of all the effects in each model is shown.

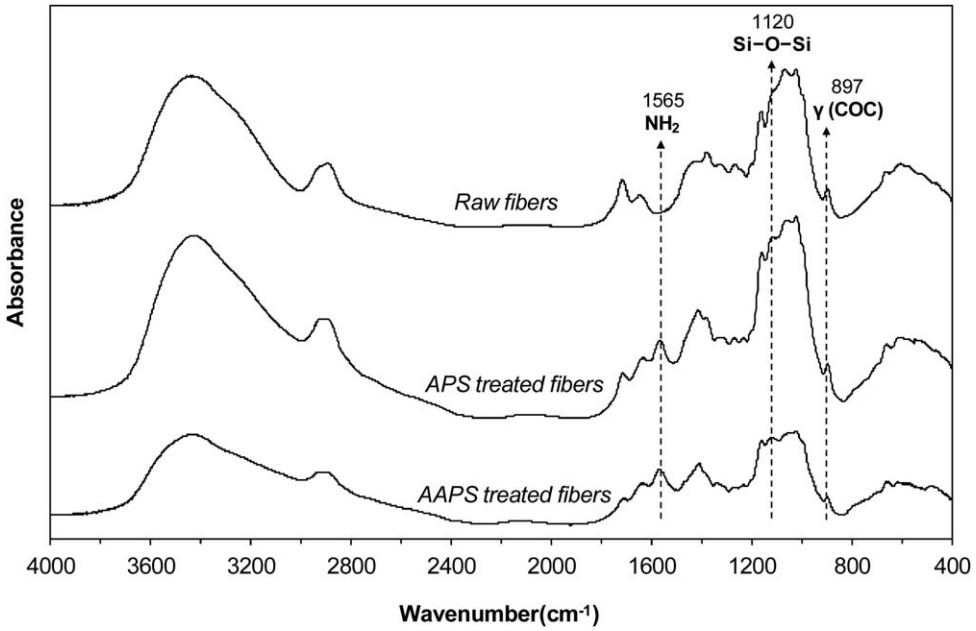

Figure 3. FTIR spectra of the raw viscose fibers and the fibers treated with the APS and AAPS silanes at the central points of the experimental designs.

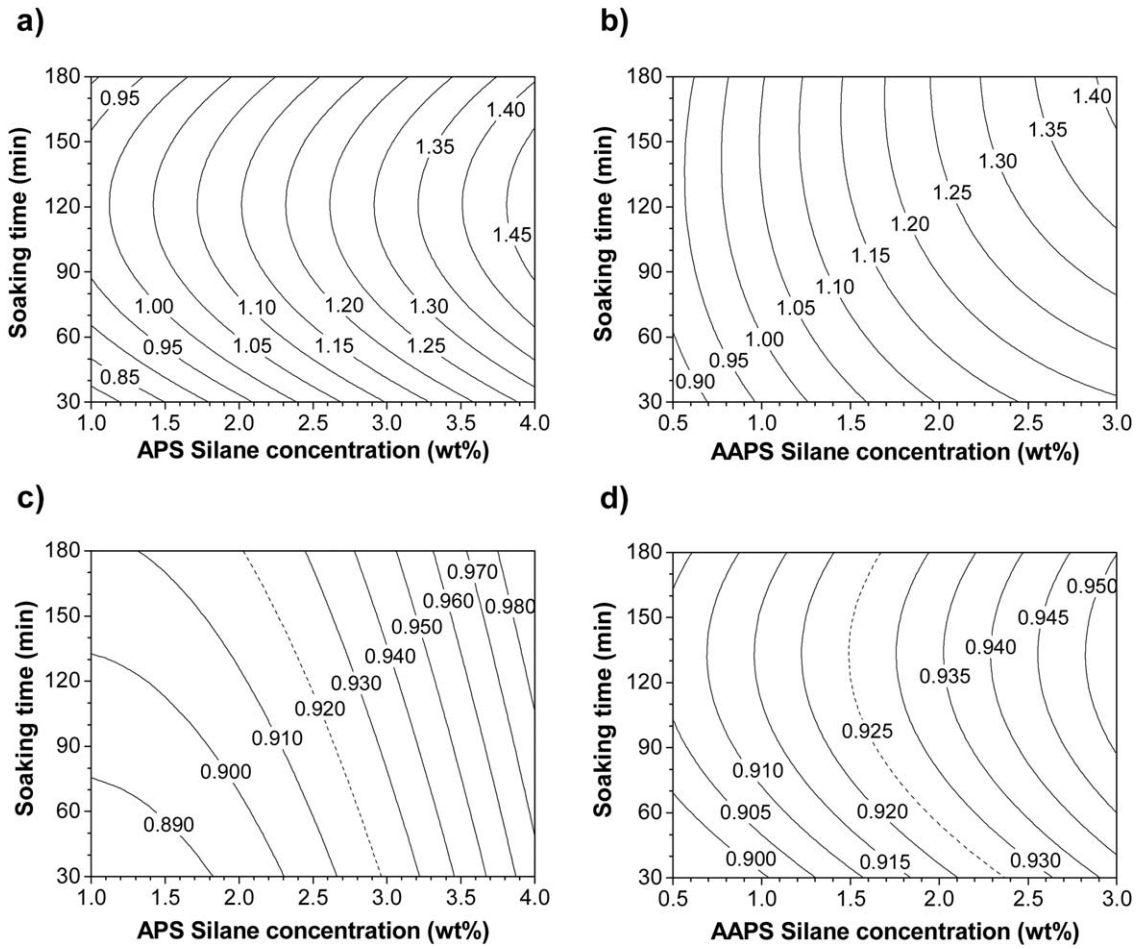

Figure 4. Contour maps for $I_{1565/897}$ of (a) APS silane and (b) AAPS silane, and $I_{1120/897}$ of (c) APS silane and (d) AAPS silane treated cellulosic fibers.

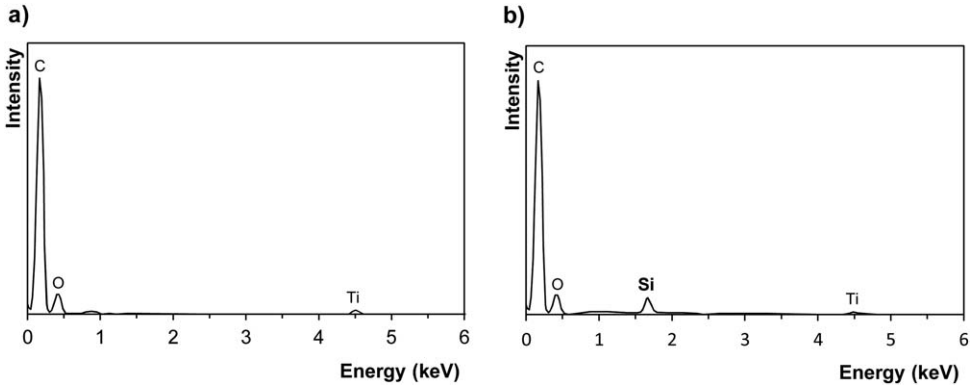

Figure 5. EDS spectra of (a) raw cellulosic fiber and (b) fiber treated with 3.5% of AAPS silane for 105 min.

The contour maps for the relative intensity $I_{1120/897}$ of the APS and AAPS silane treated fibers are shown in Figure 4(c,d), respectively. The amount of dimeric and oligomeric structures ($I_{1120/897}$) increases with the concentration of APS and AAPS silanes and with the soaking time of the fibers in the silane solutions. The influence of the silane concentration on this response is greater than that of the soaking time for both silane treatments. The $I_{1120/897}$ values in the contour maps vary in the ranges 0.890–0.980 and 0.900–0.950 for the APS and AAPS silane treatments, respectively. The intensification of the band near 1120 cm^{-1} was appreciated in the FTIR spectra above certain values of silane concentration and soaking time. Thus, 0.920 and 0.925 were set as maximum acceptable $I_{1120/897}$ values for the APS and AAPS treatments, respectively. These values are highlighted in the contour maps of the Figure 4(c,d) with dotted lines. In other words, a combination of the variables silane concentration and soaking time must be selected carefully to obtain $I_{1120/897}$ values below 0.920 and 0.925 for the APS and AAPS silane treated fibers, respectively, and thus ensure minimal formation of dimeric and oligomeric structures during the treatments.[29,32]

EDS Analysis

Elemental analysis through EDS allowed determining the semi-quantitative silicon amount incorporated into the cellulosic fibers after the treatment (*Si*). Analysis at a point of the silane treated fiber provides the weight percentages of the elements: carbon, oxygen, titanium, and silicon. Carbon and oxygen are part of the structure of cellulose. Titanium comes from the titanium dioxide in anatase crystalline form, which is a bleaching agent widely used in the production of regenerated fibers. Silicon derives from the silane that has been incorporated into the fibers and its percentage (*Si*) provides a measure of the efficiency of the silane treatment.

EDS spectra of the raw fiber and a fiber treated with 3.5% of AAPS silane for 105 min, are shown in Figure 5(a,b), respectively. Both spectra show bands corresponding to carbon, oxygen, and titanium, which are part of the structure of cellulose and bleaching agent, as aforementioned. The main difference between the spectra was the silicon peak, which only appeared in the silane treated fibers [Figure 5(b)].

The contour maps of the silicon percentage of the APS and AAPS silane treated fibers are shown in Figure 6. Each line

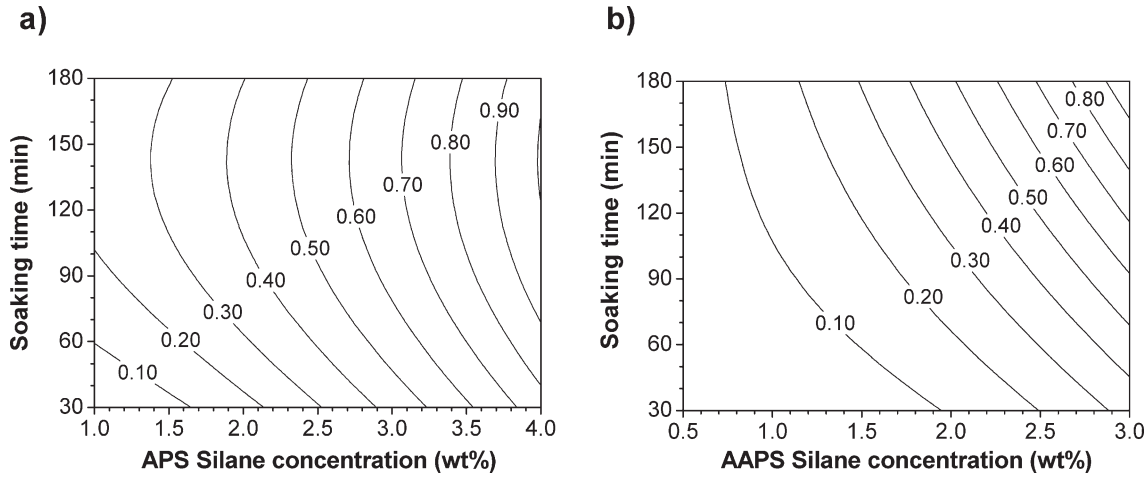

Figure 6. Contour maps for Si of (a) APS silane and (b) AAPS silane treated cellulosic fibers.

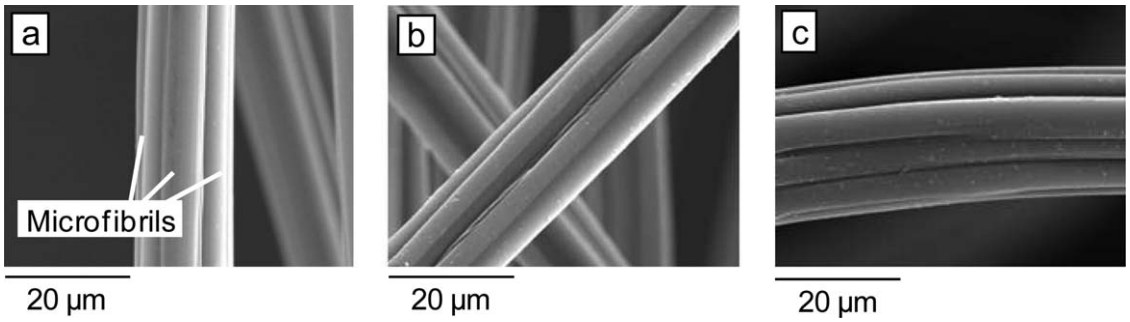

Figure 7. SEM micrographs of the viscose cellulosic fibers: (a) Raw fiber; (b) 2.5% APS silane, 105 min; (c) 1.7% AAPS silane, 105 min.

represents the combinations of soaking time and silane concentration that lead to a specific value of the percentage of silicon in the cellulosic fibers. The silane amount incorporated into the fibers during the treatments (*Si*) increases with the silane concentration employed in the modification and with the soaking time of the fibers in the silane solutions. The silicon percentage measured by EDS is more affected by the silane concentration than by the soaking time, similarly than in the contour maps of the FTIR relative intensity $I_{1565/897}$. Moreover, certain reversible hydrolysis of the APS silane can be predicted in the contour map of Figure 6(a), in accordance with the maximum found when the soaking time is increased for a given silane concentration. No evidences of reversible hydrolysis were found for the AAPS silane treatment [Figure 6(b)].

SEM Observation

Figure 7 shows the SEM images of the untreated, APS and AAPS silane treated fibers. Central points of the APS and AAPS experimental designs were chosen for the SEM images, which are representative of the whole set of samples. There are no appreciable differences between the three images, evidencing the minimal formation of dimeric and oligomeric structures in the silane treated fibers. Each fiber presented well differentiated subunits or microfibrils and the surfaces coatings created by the silanes were small enough that no significant modification could be appreciated in the APS and AAPS silane treated fibers [Figure 7(b,c)].

Optimal Conditions of the Treatments and Contact Angle Measurements

The selection of the optimal conditions of the silane treatments of the fibers was based on a compromise among achieving maximum values of the relative intensity of FTIR bands 1565/897 ($I_{1565/897}$), maximum values of the percentage of silicon determined by EDS (*Si*), and minimum values of the relative intensity of the bands 1120/897 cm^{-1} ($I_{1120/897}$). Thus, the optimal conditions of the treatments were found to be 2.2% APS for 120 min and 1.5% AAPS for 100 min. These conditions lead to an amount of each silane bonded to the fibers enough to completely coat their surfaces, but not excessively to avoid the formation of undesired dimeric and oligomeric structures during the treatments.

The predicted responses $I_{1565/897}$, $I_{1120/897}$, and *Si* for those optimal conditions were obtained employing the quadratic models, whose regression coefficients are shown in Table II. Cellulosic fibers were treated in the optimal conditions of the APS and AAPS silane treatments and experimental values of the responses were obtained in order to verify the predictions of the models. The predicted and experimental values of the responses are compared in Table III. The good correlation between predicted and experimental values (errors < 6%) confirmed that the applied models were suitable for describing the behavior of the silane treatment of the fibers.

Contact angles between the cellulosic fibers from eucalyptus wood (reinforcement) and a resol-type phenolic resin (matrix) were measured to test the ability of the silane treated fibers to be employed as reinforcement in phenolic composites. Thus, the effect of the silane treatments on the wettability of the fibers was studied. The dynamic acquisitions of the contact angle values for the raw fibers, fibers treated with 2.2% APS for 120 min, and fibers treated with 1.5% AAPS for 100 min are shown in Figure 8. The contact angles decreases from 40.4° in the raw fibers to 35.7° and 33.1° in the fibers treated with the silanes APS and AAPS, respectively. The treatment of the fibers with the silanes reduced the contact angle between the cellulosic fibers and the phenolic resin due to the improvement in the fiber wettability.

Table III. Predicted and Experimental Values of the Responses Studied for Cellulosic Fibers Treated with APS and AAPS Silanes in Optimal Conditions

	2.2% APS Silane, $t = 120$ min			1.5% AAPS Silane, $t = 100$ min		
Response	Predicted	Experimental	Error (%)	Predicted	Experimental	Error (%)
$I_{1565/897}$	1.181	1.189	0.72	1.133	1.116	1.20
$I_{1120/897}$	0.913	0.918	0.54	0.923	0.911	1.31
Si (%)	0.46	0.48	4.37	0.17	0.18	5.45

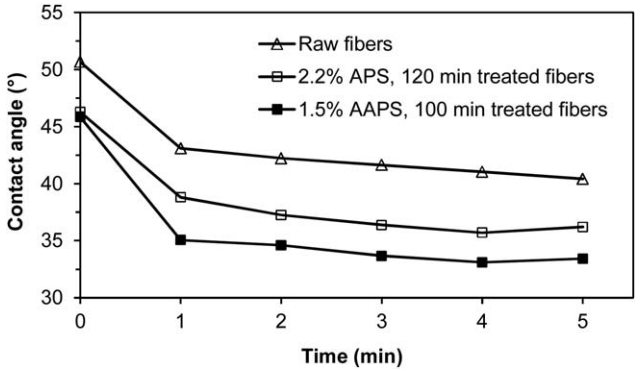

Figure 8. Contact angles for the raw cellulosic fibers, fibers treated with 2.2% APS for 120 min, and fibers treated with 1.5% AAPS for 100 min.

CONCLUSIONS

Optimization of the treatment conditions of viscose cellulosic fibers from eucalyptus wood with the silanes APS and AAPS was carried out. The application of statistical models using the ANOVA test allowed selecting the silane treatments conditions (silane concentrations and soaking times) that lead to the most effective surface modification of the fibers. The optimal silanes treatment conditions were found to be 2.2% APS for 120 min and 1.5% AAPS for 100 min. These conditions were set as a compromise solution among achieving maximum values of the amount of silane ($I_{1565/897}$) and the percentage of silicon (*Si*) in the cellulosic fibers after their treatment, and minimizing the formation of dimeric and oligomeric structures ($I_{1120/897}$). SEM images of the APS and AAPS silanes treated fibers corroborated the minimal formation of those structures. Furthermore, contact angle measurements between the fibers and a resol-type phenolic resin revealed that the silane treatment enhanced the wettability of the fibers and improved their adhesion with the phenolic matrix.

The comparison between experimental and predicted values verified the availability and the accuracy of the models applied. The experimental design methodology and the application of statistical models were valid for the optimization of the silane treatment conditions of the cellulosic fibers.

ACKNOWLEDGMENTS

The authors are grateful to the "Ministerio de Ciencia e Innovación" for financial support (project CTQ2010-15742).

REFERENCES

1. Belgacem, M. N.; Gandini, A. Monomers, Polymers and Composites from Renewable Resources; Elsevier: Oxford, **2008**.
2. Megiatto, J. D., Jr.; Ramires, E. C.; Frollini, E. *Ind. Crop. Prod.* **2010**, *31*, 178.
3. Jawaid, M.; Abdul Khalil, H. P. S. *Carbohydr. Polym.* **2011**, *86*, 1.
4. Ku, H.; Wang, H.; Pattarachaiyakoop, N.; Trada, M. *Compos. B* **2011**, *42*, 856.
5. La Mantia, F. P.; Morreale, M. *Compos. A* **2011**, *42*, 579.
6. Abdul Khalil, H. P. S.; Bhat, A. H.; Ireana Yusra, A. F. *Carbohydr. Polym.* **2012**, *87*, 963.
7. Rojo, E.; Oliet, M.; Alonso, M. V.; Del Saz-Orozco, B.; Rodriguez, F. *Polym. Eng. Sci.* **2014**, *54*, 2228.
8. Rojo, E.; Alonso, M. V.; Oliet, M.; Del Saz-Orozco, B.; Rodriguez, F. *Compos. B* **2015**, *68*, 185.
9. Kokta, B. V.; Maldas, D.; Daneault, C.; Béland, P. *J. Vinyl. Technol.* **1990**, *12*, 146.
10. Bledzki, A. K.; Gassan, J. *Prog. Polym. Sci.* **1999**, *24*, 221.
11. Eichhorn, S. J.; Baillie, C. A.; Zafeiropoulos, N.; Mwaikambo, L. Y.; Ansell, M. P.; Dufresne, A.; Entwistle, K. M.; Herrera-Franco, P. J.; Escamilla, G. C.; Groom, L. H.; Hughes, M.; Hill, C.; Rials, T. G.; Wild, P. M. *J. Mater. Sci.* **2001**, *36*, 2107.
12. George, J.; Sreekala, M. S.; Thomas, S. *Polym. Eng. Sci.* **2001**, *41*, 1471.
13. Stevens, C.; Verhé, R. Renewable Bioresources: Scope and Modification for Non-Food Applications; Wiley-Blackwell: Chichester, **2004**.
14. Wool, R. P.; Sun, X. S. Bio-Based Polymers and Composites; Elsevier: Burlington California, London, **2005**.
15. Ben Sghaier, A. E. O.; Chaabouni, Y.; Msahli, S.; Sakli, F. *Ind. Crop. Prod.* **2012**, *36*, 257.
16. Sever, K.; Sarikanat, M.; Seki, Y.; Erkan, G.; Erdoğan, Ü. H.; Erden, S. *Ind. Crop. Prod.* **2012**, *35*, 22.
17. Rojo, E.; Alonso, M. V.; Domínguez, J. C.; Del Saz-Orozco, B.; Oliet, M.; Rodriguez, F. *J. Appl. Polym. Sci.* **2013**, *130*, 2198.
18. Tan, F.; Qiao, X.; Chen, J.; Wang, H. *Int. J. Adhes. Adhes.* **2006**, *26*, 406.
19. Xie, Y.; Hill, C. A. S.; Xiao, Z.; Militz, H.; Mai, C. *Compos. A* **2010**, *41*, 806.
20. Serier, A.; Pascault, J. P.; Lam, T. M. *J. Polym. Sci. A1* **1991**, *29*, 1125.
21. Bisanda, E. T. N.; Ansell, M. P. *J Mater. Sci.* **1992**, *27*, 1690.
22. Abdelmouleh, M.; Boufi, S.; Belgacem, M. N.; Dufresne, A.; Gandini, A. *J. Appl. Polym. Sci.* **2005**, *98*, 974.
23. Lu, J.; Askeland, P.; Drzal, L. T. *Polymer* **2008**, *49*, 1285.
24. Yuan, H.; Wang, C.; Zhang, S.; Lin, X. *Appl. Surf. Sci.* **2012**, *259*, 288.
25. Pickering, K. L.; Abdalla, A.; Ji, C.; McDonald, A. G.; Franich, R. A. *Compos. A* **2003**, *34*, 915.
26. Chun, K. S.; Husseinsyah, S.; Osman, H. *Polym. Res.* **2012**, *19*, 1.
27. Matuana, L. M.; Woodhams, R. T.; Balatinecz, J. J.; Park, C. B. *Polym. Compos.* **1998**, *19*, 446.
28. Valadez-Gonzalez, A.; Cervantes-Uc, J. M.; Olayo, R.; Herrera-Franco, P. J. *Compos. B* **1999**, *30*, 321.
29. Valadez-Gonzalez, A.; Cervantes-Uc, J. M.; Olayo, R.; Herrera-Franco, P. J. *Compos. B* **1999**, *30*, 309.
30. Castellano, M.; Gandini, A.; Fabbri, P.; Belgacem, M. N. *J. Colloid. Interface Sci.* **2004**, *273*, 505.
31. Redondo, S. U. A.; Radovanovic, E.; Gonçalves, M. C.; Yoshida, I. V. P. *J. Appl. Polym. Sci.* **2002**, *85*, 2573.

32. Abdelmouleh, M.; Boufi, S.; Belgacem, M. N.; Duarte, A. P.; Ben Salah, A.; Gandini, A. *Int. J. Adhes. Adhes.* **2004**, *24*, 43.
33. Crandall, J. K.; Morel-Fourrier, C. *J. Organomet. Chem.* **1995**, *489*, 5.
34. Daniels, M. W.; Francis, L. F. *J. Colloid. Interface Sci.* **1998**, *205*, 191.
35. Beari, F.; Brand, M.; Jenkner, P.; Lehnert, R.; Metternich, H. J.; Monkiewicz, J.; Siesler, H. W. *J. Organomet. Chem.* **2001**, *625*, 208.
36. Bledzki, A. K.; Jaszkiewicz, A.; Scherzer, D. *Bioplast. Mag.* **2008**, *3*, 12.
37. Ganster, J.; Fink, H. P.; Pinnow, M. *Compos. A* **2006**, *37*, 1796.
38. Bledzki, A. K.; Jaszkiewicz, A.; Scherzer, D. *Compos. A* **2009**, *40*, 404.
39. Bledzki, A. K.; Jaszkiewicz, A. *Compos. Sci. Technol.* **2010**, *70*, 1687.
40. Vu-Manh, H.; Öztürk, H. B.; Bechtold, T. *Carbohydr. Polym.* **2010**, *82*, 761.
41. Samal, R. K.; Panda, B. B.; Rout, S. K.; Mohanty, M. *J. Appl. Polym. Sci.* **1995**, *58*, 745.
42. Matías, M. C.; De La Orden, M. U.; González, C.; Martínez, J. *J. Appl. Polym. Sci.* **2000**, *75*, 256.
43. Chiang, C. H.; Ishida, H.; Koenig, J. L. *J. Colloid. Interface Sci.* **1980**, *74*, 396.
44. Brochier, M. C.; Abdelmouleh, M.; Boufi, S.; Belgacem, M. N.; Gandini, A. *J. Colloid. Interf. Sci.* **2005**, *289*, 249.
45. Miller, J. D.; Hoh, K.-P.; Ishida, H. *Polym. Compos.* **1984**, *5*, 18.
46. Britcher, L. G.; Kehoe, D. C.; Matisons, J. G.; Swincer, A. G. *Macromolecules* **1995**, *28*, 3110.
47. Li, X.; He, L.; Zhou, H.; Li, W.; Zha, W. *Carbohydr. Polym.* **2010**, *87*, 2000.